Available online at www.sciencedirect.com
SCIENCE DIRECT®
Journal of Nuclear Materials 344 (2005) 274–280
journal of nuclear materials
www.elsevier.com/locate/jnucmat

Distributions of volatile fission products in or near the fuel-cladding gap of the FBR MOX fuel pins irradiated to high burn-up

Koji Maeda [a,*], Kosuke Tanaka [a], Takeo Asaga [a], Hirotaka Furuya [b]

[a] *Fuels and Materials Division, O-arai Engineering Center, Japan Nuclear Cycle Development Institute 4002, Narita, O-arai-machi, Ibaraki 311-1393, Japan*
[b] *Kyushu University, 6-10-1, Hakozaki, Higashi-ku, Fukuoka 812-8581, Japan*

Abstract

Distributions of volatile fission products and microstructures were studied at different axial positions in or near the fuel-cladding gap of FBR MOX fuel pins irradiated up to pin average burn-up of 110.6 GWd/t. It was found that most of the volatile fission products such as Cs, Mo, and Te were released from the fuel matrix into the fuel-cladding gap, and then they axially migrated up and down to a low temperature region along the temperature gradient. As a result, agglomerates of fission products, known as JOG (Joint Oxyde Gaine), were dispersed in the high temperature axial gap region and were densely precipitated in the low temperature axial gap region. The microstructures of MOX fuel near the gap were restructured by the irradiation as follows. In the low temperature rim region, a re-crystallized sub-micron grain structure was observed just like in irradiated LWR fuel. In the high temperature rim region, a white ring region developed which was free from voids and had large sized grains.

1. Introduction

In order to realize the burn-up extension which is of vital importance to FBR MOX fuel, it is necessary to know the fuel pin performance parameters in detail. Large amounts of volatile fission products migrate from the fuel matrix to the fuel-cladding gap in fuel pins under irradiation, and then accumulate and react there with each other and with fuel constituents. Therefore, chemical behaviors of volatile fission products in or near the fuel gap are among the most important phenomena affecting the integrity and lifetime of fuel pins, since they have significant effects on heat transfer across the gap and the FCCI (fuel-cladding chemical interaction).

A number of papers on the chemical behaviors of fission products have been published. The chemical forms of fission products mainly from thermodynamic data have been theoretically investigated by many authors [1–8]. Kleykamp [9] has carried out a comprehensive review on chemical forms of all kinds of fission products. Tourasse et al. [10] have reported the chemical forms and distributions of fission products in the Phenix fuel irradiated to high burn-up.

* Corresponding author. Tel.: +81 29267 4141; fax: +81 29 267 7130.
E-mail address: k-mae@oec.jnc.go.jp (K. Maeda).

0022-3115/$ - see front matter © 2005 Elsevier B.V. All rights reserved.
doi:10.1016/j.jnucmat.2005.04.054

2. Experimental

Fuel specifications and irradiation data of the fuel pins are follows. PuO_2 content in an MOX (mixed oxide) fuel pellet of 85% TD was 30 wt% and its O/M is 1.96. The cladding tube of 20% cold worked PNC-316 stainless steel is 6.5 mm in diameter and 0.47 mm thick, and the diametrical fuel-cladding gap was 0.16 mm. The fissile column extended 550 mm in accordance with the core length. The fuel pins were irradiated in a subassembly in JOYO up to the fuel pin peak burn-ups of 128 GWd/t. Maximum linear heat rating of fuel pins was 33.0 kW/m.

Both non-destructive and destructive post irradiation examinations were carried out. The gross γ-ray activity was measured along the axial direction of the fuel pin, together with the activities of individual nuclides such as ^{137}Cs, ^{106}Rh, and ^{103}Ru, in order to determine the distributions of burn-up and the elements noted above. After the pin puncture test, fuel pins were sectioned at different axial positions for metallographical observation and electron probe microanalysis (EPMA). The ceramographs were obtained on the fuel cross section by optical microscopy and scanning electron microscopy (SEM).

3. Results and discussion

Results of post irradiation examinations are presented here, focusing on typical fuel pins, which express overall results in the best way.

Axial distributions of ^{137}Cs in the fuel pin are plotted in Fig. 1 as a function of the distance from the bottom of the fissile column (dfb). The thick line shows the distribution of ^{137}Cs generated by fission, which was calculated by the ORIGEN-2 code [11], and the thin line shows the one observed in the irradiated fuel pin. The ^{137}Cs generated in the middle of the high temperature region migrates down along the temperature gradient to both upper and lower regions of low temperature, resulting in the formation of ^{137}Cs peaks. No ^{137}Cs migration can be seen just below the largest ^{137}Cs peak (48.4 mm dfb) in the lower column region of the fuel pin.

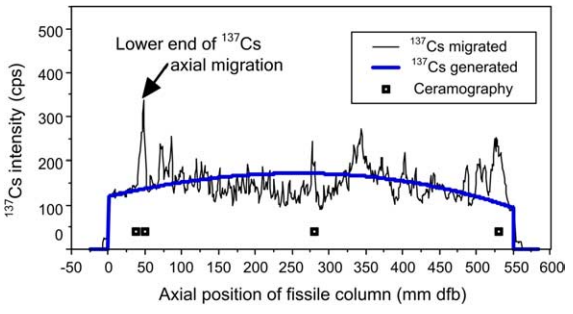

Fig. 1. Axial distribution of ^{137}Cs intensity along the fissile column of the fuel pin (pin averaged burn-up 110.6 GWd/T).

Fig. 2 shows ceramographs at several axial positions of the fuel pin shown in Fig. 1. In the axial regions below the ^{137}Cs peak (48.4 mm dfb), the fuel-cladding gap is closed and a porous fuel microstructure is evolved. In the axial region beyond the ^{137}Cs peak, an agglomerate of volatile fission products JOG (Joint Oxyde Gaine) [10] develops in the fuel-cladding gap and a fuel microstructure which is free from voids develops in the periphery. Fig. 3 shows SEM fractograph obtained adjacent to position A at 40.7 mm dfb in Fig. 2. A microstructure similar to the rim structure [12] seen in irradiated LWR fuel is observed. This means the sub-micron grain structure evolves from the as-fabricated grain structure, together with small sized pores. Fig. 4 shows EPMA mappings of position B in Fig. 2 presenting the elemental distributions in and near the fuel-cladding gap at the ^{137}Cs peak position (48.4 mm dfb). A layer of fuel matrix highly enriched in U, Pu and O is attached to the cladding inner wall. A dense precipitate of volatile fission products, which is highly enriched in Cs, Mo and O and slightly enriched in Te and Ba, is present in the region between this layer and the fuel matrix. It is most likely that large numbers of fission products, which migrate down and accumulate in this region, split the fuel matrix near the cladding along the axial direction and insert themselves into the matrix-cladding interface. In a small part of the gap region of position C at 278.3 mm dfb in Fig. 2, a dense agglomerate of fission products JOG was deposited. In the rest of the fuel-cladding gap region, however, small sized fission products agglomerates were loosely dispersed. The EPMA mapping of the dense JOG is shown in Fig. 5. There are high concentrations of Cs, Mo and O and low concentrations of Te and Ba throughout the gap, but Pd only deposits on the inner wall. And Fig. 6 shows SEM micrograph of the fuel microstructure in the rim region. Of note is a layer of the fuel microstructure which is nearly free from voids that develops throughout the rim region. This layer is called a white ring layer in this paper.

The reason for formation of this white ring layer is not fully understood yet, but the following is suggested as a formation process. In the first stage of irradiation, the temperature of the fuel surface is 800–900 °C, based on a calculation by the ESPRIT-J code [13]. Some volatile fission products are released from the high temperature fuel matrix. As the irradiation continues to 60 GWd/T, the gap width becomes small [14] and additionally the JOG of larger thermal conductivity accumulates in the fuel-cladding gap. The temperature of fuel surface decreases below 600 °C and then the rim structure appears as the fission gas accumulates in the rim region of the fuel. That is, fine grains of less than 1 μm in diameter evolve in the porous re-crystallized structure.

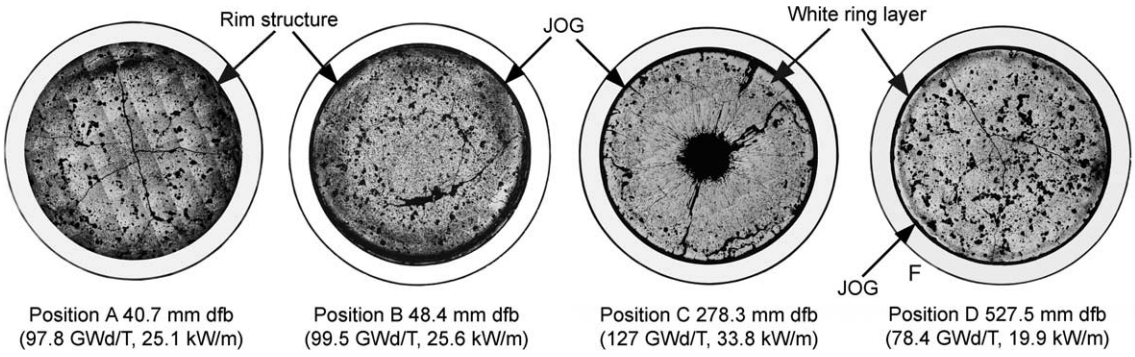

Fig. 2. Ceramographs of transverse sections in a typical fuel pin (pin averaged burn-up 110.6 GWd/T).

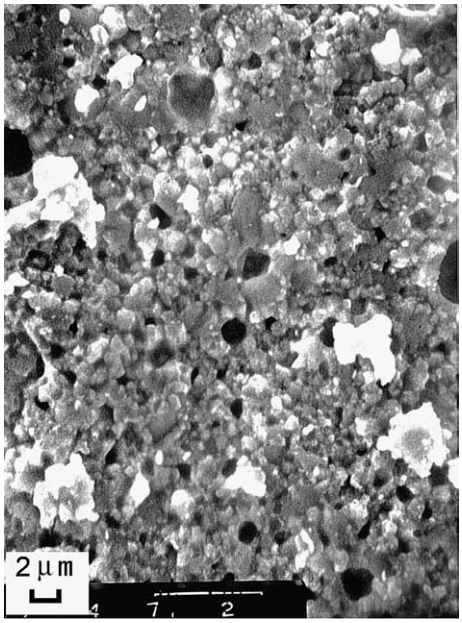

Fig. 3. SEM fractograph of the porous rim structure at fuel periphery (local burn-up 97.3 GWd/T, LHR 25.1 kW/m).

With further irradiation, the volatile fission products in the gap axially migrate to the low temperature regions along the axial temperature gradient. As a result, the gap is widened and heat conduction across the gap decreases, leading to the increase of fuel temperature.

The fission gases accumulated in the re-crystallized region are released into the gap and induce fuel densification. Both the increase of gap due to the fuel densification and increase of fission gas in the gap enhance the decrease of heat conduction. With more irradiation, the temperature in the fuel rim region exceeds 1000 °C, and most of the fission gases are released and fine grains that remain in the rim region begin to sinter.

As shown in Fig. 3, the grain sizes, and consequently the radius of curvature, are so small that the surface free energy is large. In addition, a high degree of surface roughness on the fine grains enhances the increase of surface free energy. The higher surface free energy leads to a larger sintering rate, and thus the sintering and grain growth can take place at a temperature lower than the conventional one.

Another factor to promote sintering and grain growth is the increased diffusion coefficient due to the irradiation. Matzke [15] has pointed out that the irradiation induced diffusion coefficient, D^*, is expressed by the following equation,

$$D^* = A \cdot F, \tag{1}$$

where A is a constant and F is fission rate. D^* is larger than the thermal diffusion coefficient at temperatures below 1500 °C. If the effects of both fine grains and the irradiation-enhanced diffusion coefficient on the sintering rate are considered, it is apparent that the white ring layer can be formed even at low temperature in the peripheral region of the fuel.

Fig. 7 shows the EPMA mapping for the gap region of position D at 527.5 mm dfb in Fig. 2. The ceramograph and SEM image indicate a dense JOG forms throughout the whole large fuel-cladding gap and a white ring layer develops in the rim region. The EPMA results show strong intensities of Cs, Mo and O and weak intensities of Te in the JOG. The main constituent of the cladding, Fe, can be detected on the outer surface of the fuel at an axial location near the top of the fissile column, although this element can not be observed at other axial locations. Other constituents, Cr and Ni show similar behaviors. It can be suggested from these results that the cladding components migrate in the gap toward the fuel region by a likely mechanism of cladding component chemical transport (CCCT) [3].

Fig. 8(a) and (b) show the radial distributions of Xe, Cs and Mo in the fuel matrixes at different axial positions of the fuel pin. The Xe concentration in the peripheral region decreases with the increase of relative radius, r/r_0, where r is the radius at an arbitrary position and r_0 is the radius of the fuel pellet, although the temperature

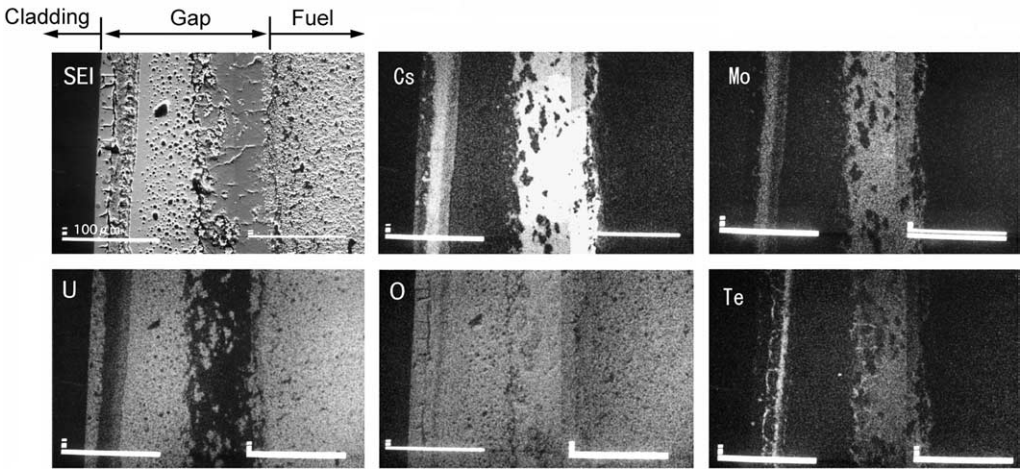

Fig. 4. EPMA mapping for the gap region of position B at 48.4 mm dfb.

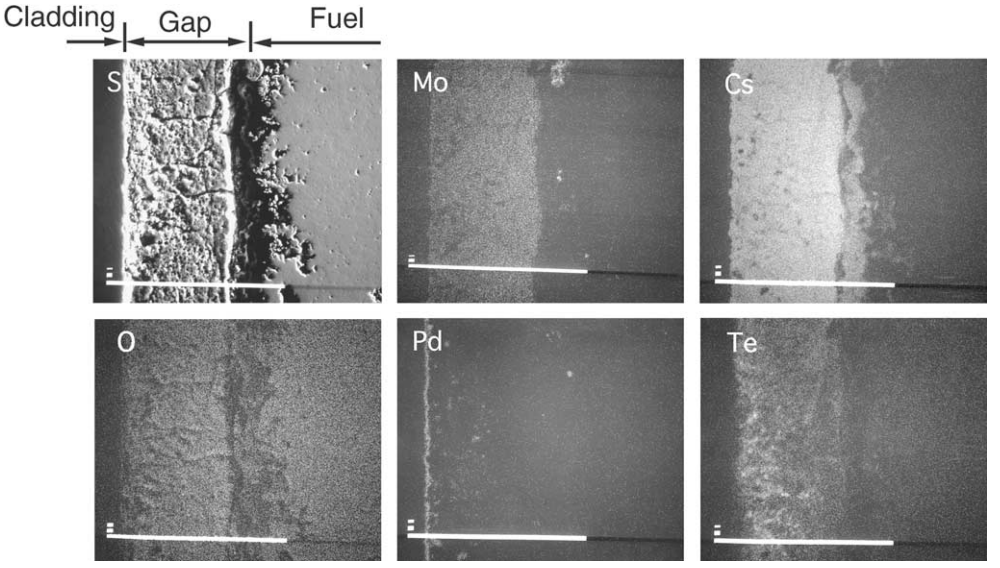

Fig. 5. EPMA mapping for the gap region of position C at 278.3 mm dfb.

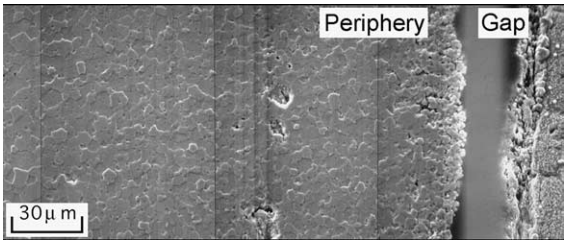

Fig. 6. SEM micrograph of restructured grain region in the fuel periphery (position C, local burn-up 127 GWd/T, LHR 33.7 kW/m).

and consequently, the release rate of Xe decrease with increasing r/r_0. As already shown in Fig. 3, the rim structure consisting of fine re-crystallized grains and pores develops in the fuel matrix near the fuel periphery. The decrease in the Xe concentration with the r/r_0 in the rim structure can be explained by the fact that a significant amount of Xe accumulates in fine pores and can not be detected by EPMA; this has been reported in studies on the fission gas release in LWR fuels [16,17]. The results in Fig. 8(b) indicate that almost all the Cs is released from the fuel matrix in the axial fuel regions irradiated at high linear heat rating (LHR), and there is little change of Cs concentration with the r/r_0. However,

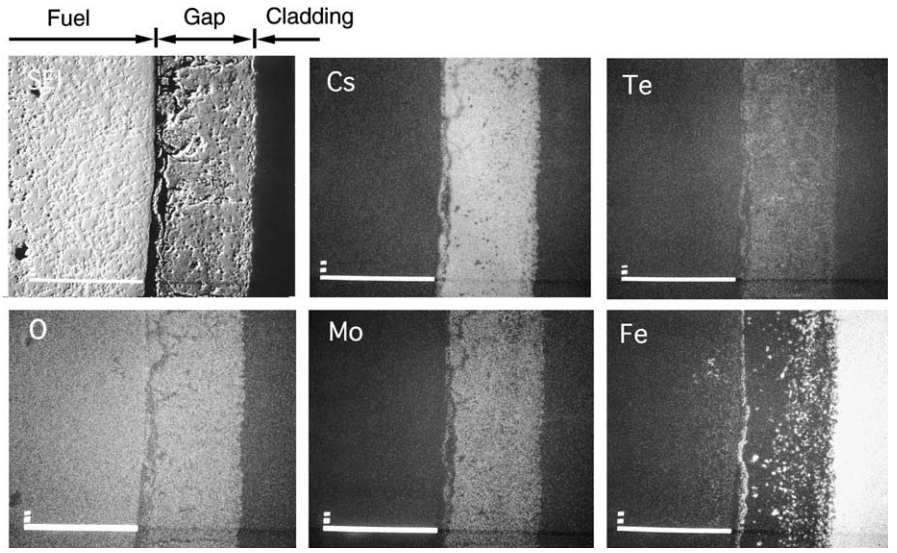

Fig. 7. EPMA mapping for the gap region of position D at 527.5 mm dfb.

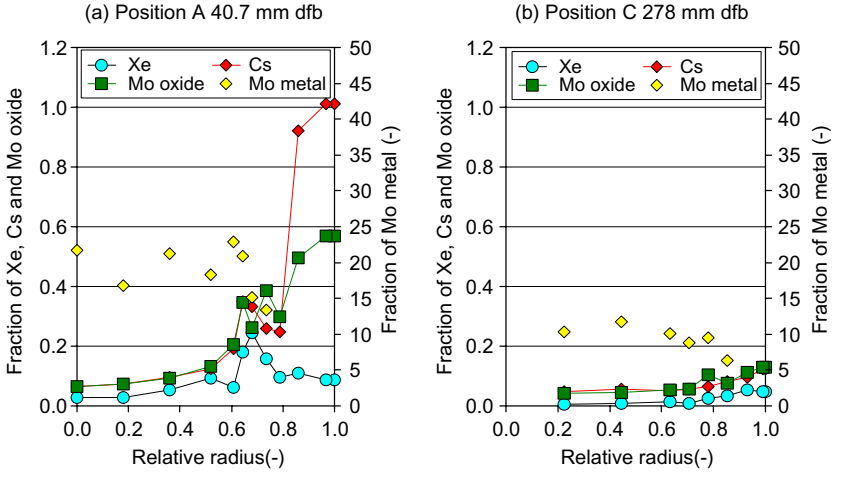

Fig. 8. Distributiion of major fission products as a function of relative radius.

Cs concentration increases in the fuel matrix in the regions irradiated at low LHR with the increase of r/r_0. Many studies have reported that Mo is present in the fuel matrix as metallic inclusions in a high temperature fuel region, based on the temperature dependence of standard formation energy of Mo oxide. As shown in Fig. 8, almost all the Mo is present in metallic Mo precipitates in the high temperature fuel region where $r/r_0 < 0.6$. In the intermediate region, $0.6 < r/r_0 < 0.75$, some of the metallic Mo is converted into Mo compounds and Mo concentration decreases with the increase of r/r_0, until finally metallic Mo disappears in the region, $r/r_0 > 0.75$. Corresponding to the change in the concentration of metallic Mo, the concentration of Mo compounds increases in the region, $0.6 < r/r_0 < 0.75$ at low LHR. On the other hand, at high LHR, its concentration is low, and shows no significant change, and the white ring layer is formed in the rim region. The behavior tendencies of both metallic Mo and Mo compounds are similar to the results already reported by other researchers [1,9].

Next, it is important to consider the relative stabilities of Cs–U–O and Cs–Mo–O compounds in the fuel-cladding gap. Fig. 9 shows the EPMA mapping which indicates the relative stabilities of Cs–U–O and Cs–Mo–O compounds in the gap which were obtained for

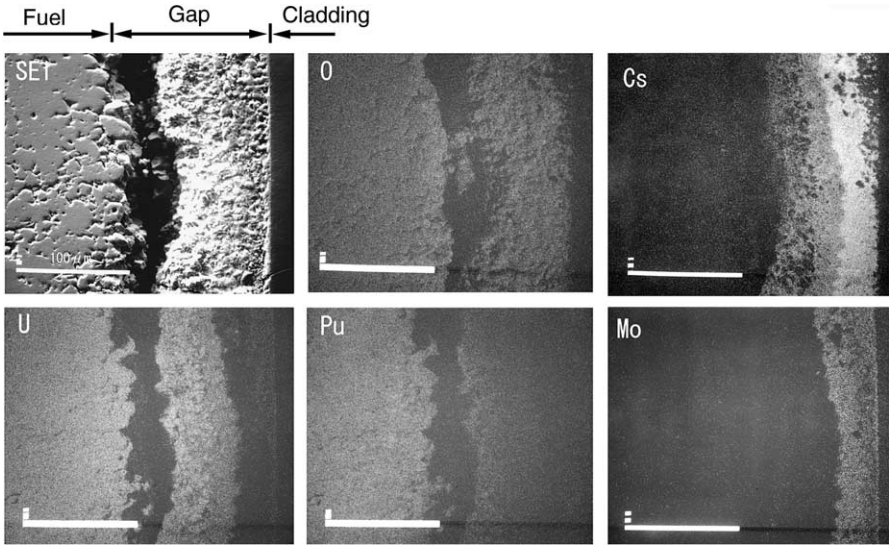

Fig. 9. EPMA mapping for the gap region at the axially central position (278 mm dfb) of another fuel pin (local burn-up 119.7 GWd/T, LHR 30.1 kW/w).

another fuel pin. In the EPMA mapping, Cs–Mo–O compounds are deposited on the inner cladding wall, while the Cs–U–O compounds are formed on the surface of the Cs–Mo–O compounds. Comparison of the Gibbs free energies of formation between Cs_2UO_4 and Cs_2MoO_4 at the temperature expected in the fuel cladding shows that the Gibbs energy of formation is lower in Cs_2UO_4 than in Cs_2MoO_4. Then, Cs_2UO_4 forms in the fuel-cladding gap early in the irradiation, and most likely by the following reaction.

$$2Cs + (U, Pu)O_2 + O_2 \rightarrow Cs_2(U, Pu)O_4$$

As the oxygen potential rises with the increase of burn-up and more Mo is released from the fuel matrix irradiated at high LHR, Cs_2 MoO_4 forms in the gap by the following equation.

$$2Cs + Mo + 2O_2 \rightarrow Cs_2MoO_4$$

Cs_2MoO_4 is more volatile than Cs_2UO_4, and thus is deposited on the cooler surface of the cladding through the porous Cs_2UO_4 layer. In addition, volatile $CsMoO_4$ migrates axially to the cooler region in the fuel-cladding gap together with other volatile species such as Cs, CsI, Te, and Pd resulting in a dense JOG formation in the fuel-cladding gap of low temperature.

4. Conclusions

Distributions of volatile fission products and microstructures were studied at different axial positions in or near the fuel-cladding gap of FBR MOX fuel pins irradiated up to 110. 6 GWd/t.

It was found that most of the volatile fission products such as Cs, Mo, and Te were released from the fuel matrix into the fuel-cladding gap, and then they axially migrated up and down to low temperature regions along the temperature gradient. As a result, agglomerates of fission products were loosely dispersed in the high temperature axial gap region and precipitated densely in low temperature regions.

From the viewpoint of relative stability of Cs–U–O and Cs–Mo–O, Cs_2MoO_4 was deposited on the cooler surface of the cladding through the porous Cs_2UO_4 layer. In addition, volatile Cs_2MoO_4 migrated axially to a cooler region in the fuel-cladding gap together with other volatile species such as Cs, CsI, Te, and Pd resulting in the gap being opened and the heat conduction being reduced across the gap.

The microstructures of MOX fuel near the gap were restructured by the irradiation as follows. In the low temperature rim region, re-crystallized sub-micron grain structure was observed just like in irradiated LWR fuel. In the high temperature rim region, the white ring region, which was free from voids and had large sized grains, developed.

Acknowledgements

The authors are grateful to Mr Y. Ohsato, Mr Y. Onuma and Mr S. Nukaga for their technical contributions to the experiments.

References

[1] E.A. Aitken, M.G. Adamson, D. Dutina, S.K. Evans, Thermodyn. Nucl. Mater. 1 (1974) 187.
[2] T.M. Bessmann, T. Lindemer, Nucl. Technol. 40 (1978) 297.
[3] M.G. Adamson, E.A. Eitken, R.W. Caputi, P.E. Potter, M.A. Mignanelli, Thermodyn. Nucl. Mater. 1 (1979) 503.
[4] O. Götzmann, J. Nucl. Mater. 84 (1979) 39.
[5] D.C. Fee, C.E. Johnson, J. Nucl. Mater. 96 (1981) 71.
[6] T. Lindemer, T.M. Bessmann, J. Nucl. Mater. 100 (1981) 178.
[7] M.G. Adamson, E.A. Aitken, T. Lindemer, J. Nucl. Mater. 130 (1985) 375.
[8] R.G.J. Ball, W.G. Burns, J. Henshaw, M.A. Mignanelli, P.E. Potter, J. Nucl. Mater. 167 (1989) 191.
[9] H. Kleykamp, J. Nucl. Mater. 131 (1985) 221.
[10] M. Tourasse, M. Boidron, B. Pasque, J. Nucl. Mater. 188 (1992) 49.
[11] A.G. Croff, ORNL-5621 (1980).
[12] C.T. Walker, T. Kameyama, S. Kitajima, M. Kinoshita, J. Nucl. Mater. 188 (1992) 73.
[13] S. Koyama, M. Osaka, T. Sekine, K. Morozumi, T. Namekawa, M. Itoh, J. Nucl. Sci. Technol. 40 (12) (2003) 998.
[14] K. Maeda, T. Asaga, J. Nucl. Mater. 327 (2004) 1.
[15] Hj. Matzke, Radiat. Eff. 75 (1983) 317.
[16] K. Nogita, K. Une, J. Nucl. Mater. 226 (1995) 302.
[17] C.T. Walker, J. Nucl. Mater. 275 (1999) 56.